EEG Information Transfer Changes in Different Daily Fatigue Levels During Drowsy Driving

Kuan-Chih Huang, Chun-Ying Tseng, and Chin-Teng Lin, *Fellow, IEEE*

***Abstract*—A significant issue for traffic safety has been drowsy driving for decades. A number of studies have investigated the effects of acute fatigue on spectral power; and recent research has revealed that drowsy driving is associated with a variety of brain connections in a specific cortico-cortical pathway. In spite of this, it is still unclear how different brain regions are connected in drowsy driving at different levels of daily fatigue. This study identified the brain connectivity-behavior relationship among three different daily fatigue levels (low-, median- and high-fatigue) with the EEG data transfer entropy. According to the results, only low- and medium-fatigue groups demonstrated an inverted U-shaped change in connectivity from high performance to poor behavioral performance. In addition, from low- to high-fatigue groups, connectivity magnitude decreased in the frontal region and increased in the occipital region. These study results suggest that brain connectivity and driving behavior would be affected by different levels of daily fatigue.**

***Index Terms*—Fatigue, brain connectivity, transfer entropy, electroencephalography (EEG).**

***Impact Statement*— This longitudinal study explores the transfer entropy of different EEG channel pairs to reveal distinct patterns of brain connectivity based on daily fatigue levels to highlight the significant factors that contribute to the detrimental effects of fatigue on driving performance.**

Manuscript received 5 December 2023; revised 19 January 2024 and 9 February 2024; accepted 11 February 2024. Date of publication 20 February 2024; date of current version 8 March 2024. This work was supported in part by the National Science and Technology Council of the Republic of China, Taiwan, under Grant NSTC 109-2221-E-009-050-MY2, Grant 110-2221-E-A49-130-MY2, Grant 112-2321-B-A49-012, and Grant 112-2221-E-A49-085, and in part by the Australian Research Council (ARC) under Discovery Grant DP210101093 and Grant DP220100803. The review of this article was arranged by Editor Laura Astolfi. *(Corresponding authors: Kuan-Chih Huang; Chin-Teng Lin.)*

Kuan-Chih Huang is with the Brain Science and Technology Center, Department of Electrical and Computer Engineering, National Yang Ming Chiao Tung University, Hsinchu 300, Taiwan (e-mail: kchuang.ece91g@g2.nctu.edu.tw).

Chun-Ying Tseng is with the Brain Science and Technology Center, National Yang Ming Chiao Tung University, Hsinchu 300, Taiwan.

Chin-Teng Lin is with Australian Artificial Intelligence Institute, Faculty of Engineering and IT, University of Technology Sydney, Sydney, NSW 2007, Australia, and also with the Brain Science and Technology Center, Department of Electrical and Computer Engineering, National Yang Ming Chiao Tung University, Hsinchu 300, Taiwan (e-mail: chin-teng.lin@uts.edu.au).

Digital Object Identifier 10.1109/OJEMB.2024.3367496

I. Introduction

THE traffic fatalities were the leading cause of death around the world [1]. According to the report, driving behavior and performance played an important role in driving safety. Therefore, to prevent car accidents and to improve traffic safety, a comprehensive understanding of the neurophysiological makers of the decline in performance during driving is critical.

Recently, many studies have investigated the different associations between brain dynamics and task performance [2], [3], [4], [5], [6], [7], [8], [9]. According to the research by Lin et al. [6] and Huang et al. [5], there are significant increases in theta power or longer episodes of theta activity, as observed by an Electroencephalography (EEG), from alert to poor performances during driving. The power of alpha, alpha+theta/beta, and alpha/beta showed an increasing trend, whereas the number of driving errors increased [2], [3], which indicated that driving performance decreased. Additionally, some studies [6], [7], [8] stated that tonic occipital alpha power and theta power increased when the reaction time increased during a long vigilance task. It was found in [4] that as reaction times increased, delta, theta, and alpha bands in the occipital and temporal cortices exhibited increasing trends in independent EEG activation. The relationship between brain dynamics and task performance varied across studies. To identify differences among the studies, our previous study [9] tracked and assessed subjects' daily fatigue variations and explored the relation between power spectrum variation in delta, theta, alpha, and beta bands with different daily fatigue levels.

Regarding the study of the brain, most previous research has focus on functional specialization, which is the analysis of regionally specific effects on the brain dividing the brain into different regions, such as the frontal, central or occipital brain regions. Distinct areas in the brain are specialized for various functions. In the recent decade, more and more research has been conducted on functional integration, which is the analysis of interregional effects on the brain. This kind of analysis is used to understand how each brain region processes information and affects responses in the entire brain network.

Functional connectivity and effective connectivity are two different aspects of the communication and interaction between different brain regions. Functional connectivity [10], [11], [12], [13], [14] denotes the statistical correlations between brain regions and demonstrates the interaction between different brain

regions. However, it doesn't necessarily imply direct communication but rather coherence across brain regions.

Recent research has introduced novel approaches to studying functional connectivity, including using the phase lag index (PLI) to estimate functional connectivity [15]. Additionally, innovative deep learning architectures [16] have been proposed for analyzing brain functional connectivity.

Otherwise, some studies have suggested the neural mechanism of effective connectivity [8], [12], [17], [18], [19], [20]. Effective connectivity represents a form of directed connectivity across brain structures, revealing causal interactions between distinct brain regions [10], [12]. The calculation of effective connectivity allows us to comprehend the flow of information across various brain areas.

In the earlier studies, Granger causality (GC) [21] and its extensions, such as directed transfer function (DTF) [17], [19] and partial directed coherence (PDC) [19], [22], [23], and related concepts such as Transfer entropy (TE), are used to study functional and effective connectivity in cognitive neuroscience [12], [17], [18], [19]. The GC analysis, however, has some prerequisites for being applied to EEG signals [12], and may not be the best method for calculating the effective connectivity of brain-related signals, which are nonlinear and non-Gaussian distributions [24], [25].

Therefore, in this study, we applied TE, a model-free measure of effective connectivity based on information theory [26], to improve the detectability of effective connectivity in nonlinear interactions. As part of our preliminary research, TE has been applied to observe the brain connectivity associated with fatigue while driving [27].

Furthermore, in regard to the brain-behavior relationship in driving, some relevant studies have focused on the neural suppression or activation of cellular potentials, on brain activity, or on blood concentrations in specific brain regions with the view of functional specialization. However, evidence [28], [29], [30] has indicated that drowsy driving may involve the coupling of different brain regions. Another piece of research suggested that the change in the brain connectivity of a specific cortico-cortical pathway may also be a sensitive neurophysiological signature for changes in alertness [30]. Furthermore, investigating the information flow between brain regions helps us reveal the coupling of synchronized, correlated systems in the brain.

According to our previous studies [5], [6], [7], [8], [9], fatigue affects the relation between the EEG spectral power in specific brain regions and behavior during simulated driving. In addition, several studies [31], [32], [33] have suggested that the network of the brain may also change between different states. Furthermore, our previous study [9] has also mentioned that the various daily fatigue levels would lead to different relations of the changes in the EEG power spectrum and behaviors during drowsy driving.

However, whether the variation in daily fatigue levels affects the specific brain regions' connectivity magnitudes during driving remains an unresolved issue of the human brain-behavior model. In this sense, we hypothesized that driving or real-world performance decrements may be associated with brain connectivity fluctuations between different modes and applied the transfer entropy method to calculate the effective connectivity of a prelabeled dataset. To identify the effect of realistic fatigue on the brain connectivity-behavior relationship during driving, the aims of the study are listed as the following: 1) to divide subjects' daily performance into three classes based on different daily fatigue levels; 2) to apply the transfer entropy (TE) method to calculate the connectivity of each piece of EEG data; and 3) to inspect the fluctuations in connectivity with the changes in driving performance among three daily fatigue.

II. Materials and Methods

A. Subjects and EEG Acquisition

Sixteen healthy subjects aged 20–26 (11 males and five females) were recruited to join the study. All participants were scheduled to conduct the lane-keeping task at each of three daily fatigue levels (high-, medium-, and low-fatigue) and explore the effect of different daily fatigue levels on simulated driving performance and corresponding informative EEG features. This means that each subject experimented while they were at three different individual daily fatigue levels. Each subject's daily fatigue level was divided according to the statistical distribution of daily effectiveness scores recorded using ReadiBand actigraph (Fatigue Science, Vancouver, BC) for at least one continuous 1 month (details are presented in Section II-B). This experimental paradigm was adapted from our previous methods [9]. The subjects were also required to complete subjective questionnaires to check psychometric responses to fatigue, sleep, and stress, including the Karolinska Sleepiness Scale (KSS) [34], [35] and the Fatigue Visual Analog Scale (FVAS) [36], during each experimental session to ensure daily fatigue level accuracy. They are right-handed and have the normal or corrected-to-normal vision, and have not taken any medication that affects cognitive function.

In this study, the behavioral data were recorded and monitored during the whole process of the experiment. EEG data were recorded from Ag/AgCl electrodes, placed according to the modified international 10–20 system, by the Synamp system (Compumedics Ltd., VIC, Australia) during the task. The contact impedance between all the electrodes and the skin was kept under 10 kΩ. The EEG signal was recorded at a sampling rate of 1000 Hz.

This study was carried out in strict accordance with the recommendations in the Guide for Committee of Laboratory Care and Use of the National Chiao Tung University. The Institutional Review Board of National Chiao Tung University approved the protocol. Each participant read and signed an informed consent form before the experiment began.

B. Daily Fatigue Level Determination

The ReadiBand actigraph (Fatigue Science, Vancouver, BC) was given to each subject. It is a wrist-worn actigraphy device that records the duration, quantity and quality of sleep automatically and objectively. By means of the patented Sleep, Activity, Fatigue, and Task Effectiveness model (SAFTE) [37], the ReadiBand can evaluate the estimated effectiveness score.

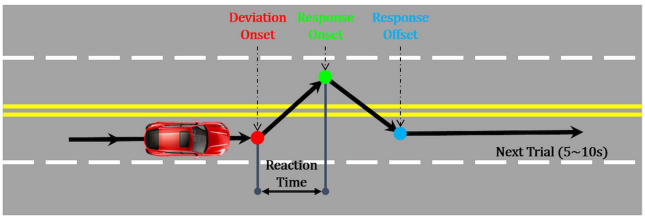

Fig. 1. Event-related lane departure paradigm. The solid black arrows represent the driving trajectory. The red point represents the deviation onset. The green point represents the response onset. The blue point represents the response offset. The driver's reaction time (RT) is the time interval from the deviation onset (red point) to the response onset (green point). The next deviation begins 5–10 s after the response offset (adapted from Ref. [5] and [6]).

The SAFTE model calculates and simulates the physiological processes of the human body. It can determine the level of daily fatigue using the effectiveness score mentioned above at any given point in time. It contains a sleep-reservoir process that represents the method in which recovery sleep is affected by bed time, wake time, sleep quantity and quality, sleep debt, and the circadian timing of sleep, as well as any type of sleep fragmentation. Additionally, it contains a circadian process that simulates the way in which the body clock influences circadian regulation and performance. The real-time effectiveness scores (ES, 0%–100%) are provided by the SAFTE model. Using these scores, the model will make a decision as to which level of daily fatigue the subject is at. According to effectiveness scores, the levels of daily fatigue are divided into three levels (high-, medium- and low-fatigue) and marked as three different risk groups of accident (high-risk, reduced and normal group, respectively). The normal group as having an effectiveness score near the MEAN + standard deviation (SD) (SD; The MEAN and SD were calculated over approximately 1 month). Subjects with effectiveness scores lower than the MEAN – SD were considered the high-risk group. Those with effectiveness scores lying between the normal and high-risk ranges were categorized as the reduced group. Participants were asked to wear the actigraph continuously for the duration of the study [9].

C. Lane-Keeping Task

An event-related lane departure paradigm was implemented using a virtual-reality scene in Fig. 1, adapted from our previous studies [5], [6]. In the scene, the speed of the vehicle was 100 km/hr, and it would drift away automatically from the original cruising lane to the right or left side at random. The subjects were required to steer the automobile back to the original lane as fast as possible after they perceived the deviation. If the subjects did not respond to the perturbation of the vehicle, it would hit the right or left curb of the roadside after 2.5 or 1.5 seconds, respectively. The vehicle would keep moving along the roadside until it was steered back to the original lane. The lane departure event is regarded as a trial that is composed of three significant moments. The deviation onset represents the moment when the vehicle starts to drift away the original lane. The response onset indicates the moment when the participant has feels the car perturbation and begins to rotate the steering wheel. Finally, the response offset represents the moment when the vehicle is steered back to the original lane, and the participant stops moving the steering wheel. The reaction time is defined as the interval between the response onset and the deviation onset. The next trial occurs 5 to 10 seconds after every response onset. The duration time for each task session is around one hour, including 300 trials at least. There were not any another stimuli during the driving task that would create a car condition that would induce the driving fatigue of the subjects. The cognitive states of the subjects were recorded using a real-time camera, as well as the driving trajectory throughout the session.

D. Connectivity Estimation by Transfer Entropy

Schreiber [26] proposed an information-theoretic measure termed transfer entropy (TE). TE is derived from the conditional mutual information and conditional transition probabilities between any two processes evolving in time. This measure supposes that $X = \{x_1, x_2, \cdots, x_n\}$ and $Y = \{y_1, y_2, \cdots, y_n\}$ are two processes that represent two interacting systems (time series, n is the number of time bin of process) that can be approximated by stationary Markov processes. Let $x_t^d = \{x_t, x_{t-\tau}, x_{t-2\tau}, \cdots, x_{t-(d-1)\tau}\}$ be an embedding vector that is related to the full state of the processes of interest. The dimension of the embedding space is d, and the delay is τ [18]. Under the assumption that the system can be approximated by a stationary Markov process of order d, the transition probabilities that describe the system are as follows:

$$p\left(x_{t+1} \left| x_t^d \right.\right) \tag{1}$$

The entropy rate of a system X is the amount of additional information that is required to represent the value of an additional state. All previous states of the system are known and can be computed as follows:

$$H\left(x_{t+u} \left| x_t^d \right.\right) = -\sum_{x_{t+u}, x_t^d} p\left(x_{t+u} \left| x_t^d \right.\right) \log p\left(x_{t+u} \left| x_t^d \right.\right) \tag{2}$$

where u is the prediction time, and $p(*)$ is the probability. The probabilities can be estimated via kernel estimation or by the k-nearest neighbor approach [12], [26], [38]. We wanted to measure the amount of information transferred from process Y to process X. The entropy rate of a system X is the amount of additional information that is required to represent the value of an additional state of the system X and the other system Y. All previous states are known and can be computed as follows:

$$H\left(x_{t+u} \left| x_t^d, y_t^m \right.\right) = -\sum_{x_{t+u}, x_t^d} p\left(x_{t+u} \left| x_t^d, y_t^m \right.\right) \log p\left(x_{t+u} \left| x_t^d, y_t^m \right.\right) \tag{3}$$

If the two processes are independent, there is no transfer of information, and $p(x_{t+u}|x_t^d) = p(x_{t+u}|x_t^d, y_t^m)$, that also is $H(x_{t+u}|x_t^d) = H(x_{t+u}|x_t^d, y_t^m)$, where the state of X only depends on d states of X. As proposed by Schreiber [26], a measure of the deviation from this generalized Markov property can be computed using the Kullback-Leibler divergence or by

mutual information. This measurement is a directed measure of the information flow from Y to X and is called the transfer entropy, $TE(Y \to X)$and is computed as follows [12], [26], [39]:

$$TE\left(Y \to X\right) = H\left(x_{t+u} \left| x_t^d\right.\right) - H\left(x_{t+u} \left| x_t^d, y_t^m\right.\right)$$
$$= \sum p\left(x_{t+u}, x_t^d, y_t^m\right) \log \frac{p\left(x_{t+u} \left| x_t^d, y_t^m\right.\right)}{p\left(x_{t+u} \left| x_t^d\right.\right)} \quad (4)$$

The essence of the calculation of transfer entropy is directional and dynamic information transfer. We can recognize TE as an asymmetric measure and see its property of causality detection, which means $TE(Y \to X) \neq TE(X \to Y)$. Under the assumption that the processes are independent from each other, $TE(Y \to X) = TE(X \to Y) = 0$.

The estimation of parameters and the calculation of TE were performed by TRENTOOL (version 2.0.4) [40], which is an open source toolbox for Matlab that analyzes information flow in a time series with transfer entropy. The algorithms used to determine the appropriate time delay (τ) was proposed by Cao [41] based on false neighbors computation and an alternative known as the Ragwitz' criterion [42], while the dimension (d and m) was obtained using an effective search algorithm [12], [40]. With the TRENTOOL toolbox, the range of embedding dimensions (d and m) is scanned from 1 to 10 to find the optimal dimension.

E. EEG Processing and TE Analysis

The EEG data were preprocessed and then applied the transfer entropy method to calculate the effective connectivity. Then, we combined the reaction times with the effective connectivity to observe the connectivity between different brain regions during driving. All EEG data were applied a bandpass filter ranging from 0.5 Hz to 50 Hz to remove the DC noise and the high-frequency noise, and then through downsampling from 1000 Hz to 250 Hz to minimize the computational complexity. An epoch refers to a segment of multichannel EEG signals that is time-locked to some special kind of event. In order to observe the EEG dynamics during a specific event, epoch extraction was conducted by cutting the nine seconds of continuous EEG data ranging from two seconds before the deviation onset to the seven seconds after the deviation onset.

Tonic EEG dynamics refer to the changes in spontaneous EEG activity that are associated with the long-term changes in baseline arousal levels [4]. In our research, we wanted to investigate the tonic EEG dynamics during driving. Therefore, we analyzed the EEG data from 2 s before the deviation onset of each epoch.

To reduce the intrinsic inter-subject and intra-subject differences of each experiment session, the TE values of each session were normalized by subtracting their own TE baseline. The TE baseline was calculated as the mean of the TE from 10% of the sorted RTs in each subject. Therefore, the normalized TE represented the changes in TE relative to the baseline TE. In addition, the RT was divided by the mean of the 10% of the sorted RTs for each session to obtain the normalized RT. The normalized RT enabled us to observe the connectivity dynamics during the changes in driving performance. Then, all the results for each subject were combined together and sorted from the best to worst RT. The TE values were smoothed by moving the average filter (window size: 1 unit of RT; step size: 0.1 unit of RT) to obtain the TE connectivity dynamics.

In this study, all the data were divided into three groups (high-risk, reduced, and normal group) based on different levels of daily fatigue and were transformed into three kinds of TE connectivity dynamics. Furthermore, this study compared the EEG connectivity changes between any two levels of daily fatigue. In this case, Wilcoxon signed-rank tests were performed to test the pairwise comparison between any two groups of TE values. The false discovery rate (FDR) was furthered used to obtain the FDR-adjusted p-values. Additionally, this study's experimental trial numbers for each daily fatigue level were high-risk state: 4025, reduced state: 4588, and normal state: 4716, respectively. That is the number of TE values of each state for each EEG channel pair.

Previous studies [5], [6] have stated that the independent EEG components, including the frontal, central, left motor, right motor, parietal and occipital regions, are highly correlated with fatigue and behavioral lapse. The brain regions mentioned above play important roles in the brain-behavior relationship during driving. Our goal was to observe the information flow among different brain regions during driving using EEG channels. In this study, we follow our previous studies [9], [27] to compare with brain connectivity of different brain regions. The EEG channels used were those that were the closest to the main brain regions mentioned above. They were Fz (frontal region), Cz (center region), C3 (left motor region), C4 (right motor region), Pz (parietal region), and Oz (occipital region).

III. Results

A. Baseline TE Among Different Levels of Daily Fatigue

Within each level of daily fatigue, the mean TE of the trials with the shortest RTs (first 10% of all RT-sorted trials) was as the baseline TE and calculated the average baseline TE of all the subjects. Fig. 2 shows the average baseline TE among different levels of daily fatigue (vertical axis, average baseline TE between all pairs of channel; horizontal axis, three levels of daily fatigue; Color: red, high-risk state; green, reduced state; and blue, normal state). For each pair of channels, the standard deviation of the average baseline TE across the three levels of daily fatigue was enormous. Although subtle differences in the baseline TE values among the different levels of daily fatigue were found in some channel pairs with the naked eye, there were no statistically significant differences in the baseline TE values among the different levels of daily fatigue.

B. Reaction Time (RT)-Sorted EEG Connectivity Changes

Fig. 3 shows the EEG connectivity changes among channel pairs across three groups (high-risk, reduced, and normal) (vertical axis, TE values between all pairs of channels; horizontal

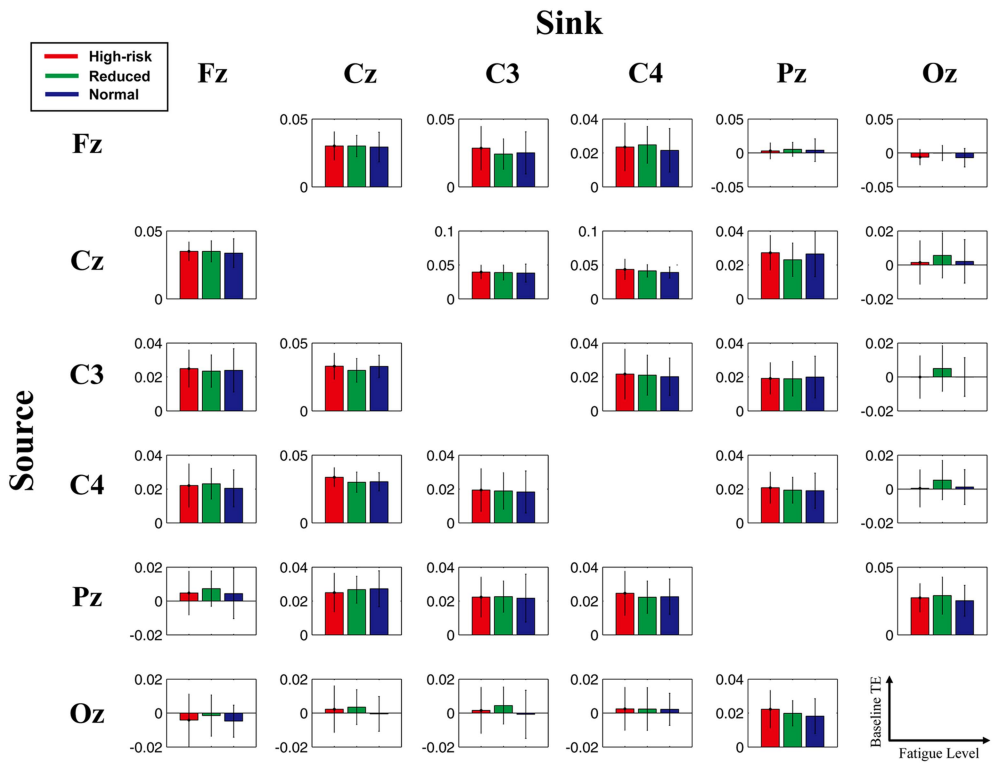

Fig. 2. Comparison of baseline TE values between channel-pairs across the three different daily fatigue level groups. The red, green, and blue bars are high-risk, reduced, and normal groups, respectively. Standard deviations are also shown.

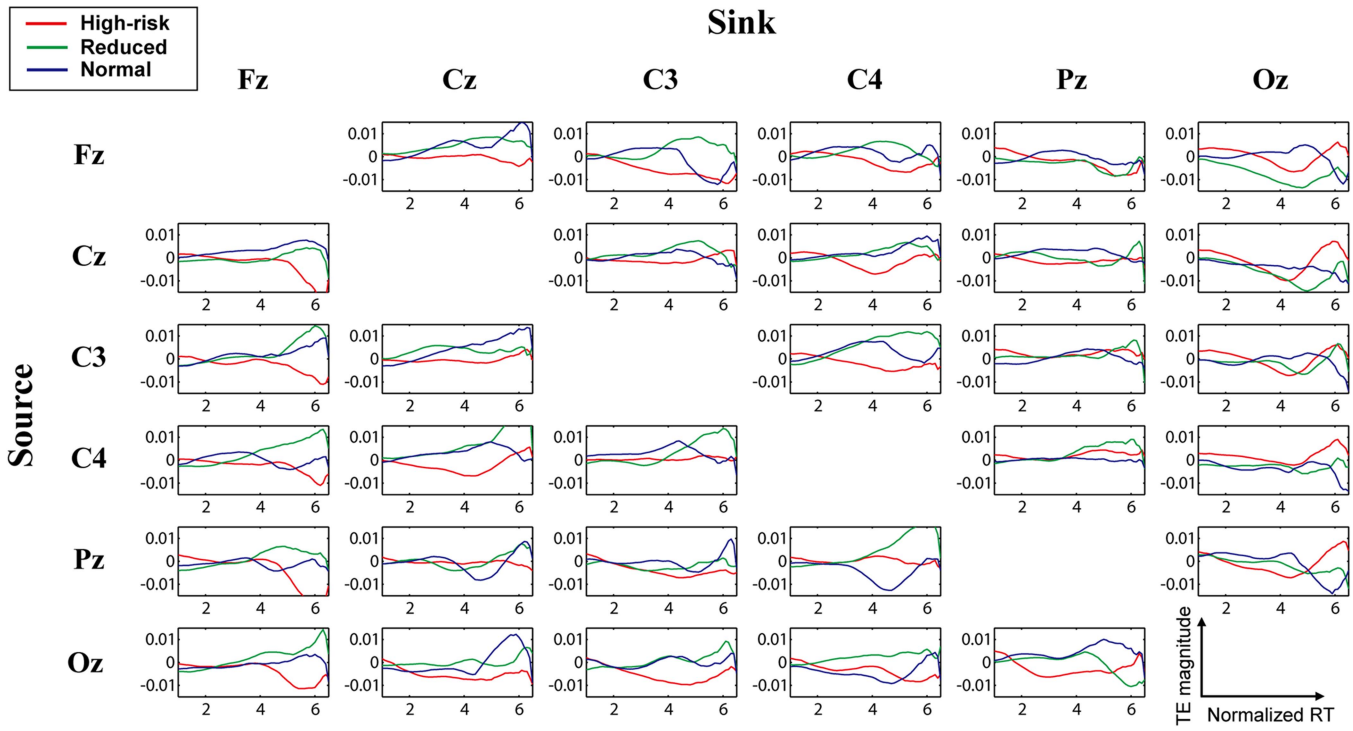

Fig. 3. Connectivity magnitudes between pairs of EEG channels (Fz, Cz, C3, C4, Pz, and Oz) estimated by transfer entropy among the three different daily fatigue level groups. The red, green and blue curves represent high-risk, reduced and normal groups, respectively.

axis, sorted normalized RT), where causality is from row to column. All measures were smoothed using a window smoothing method.

The blue curves show the relation between connectivity changes and the sorted normalized RTs among channel pairs in the normal state. There were multiple trends of RT-sorted TE values at different channel pairs. TE values showed an inverted U shape in the channel pairs associated with Cz, C3, and C4, indicating motor-related channels. As well, all channel pairs whose source was Oz displayed a similar trend in connectivity. The magnitude of connectivity was an inverted U-shaped shift, which meant that the U-shape was delayed with the sorted normalized RT, and the location of the magnitude peak appeared later than the inverted U-shape discussed above. Nevertheless, different from the trend in the Oz-source channel pairs, a unique pattern was observed in the channel pairs whose sink were Oz. The magnitude of connectivity declined monotonously as the normalized RT increased. In summary, the normalized RT-sorted TE changes were considerably different among the distinct brain regions.

The green curves show the relation between connectivity changes and the sorted normalized RTs among the channel pairs in the reduced state. As with the normal state, inverted-U shaped changes in the TE values occurred in some channel pairs, including Fz-to-Cz, Fz-to-C3, Fz-to-C4 and Cz-to-C3, Pz-to-Fz. We also observed inverted-U shaped shifts at C3-to-Fz and C3-to-C4, as well as at C4-to-Fz, C4-to-Cz, C4-to-C3, Pz-to-Fz, and Pz-to-C4. The connectivity magnitude increased as the normalized RT increased, and the peak was located at RT=6, which was larger than the peak location of the TE magnitude of the inverted-U shaped shift in the normal state. The connectivity magnitude began to decrease abruptly after RTs higher than 6. Finally, there was an interesting observation that the connectivity magnitudes of all the channel pairs whose sink were Oz decreased from high normalized RTs to low normalized RTs. It can be seen that the magnitudes of connectivity changed in different brain regions.

The red curves show the relation between connectivity changes and the sorted normalized RTs among channel pairs in the high-risk state. The connectivity magnitudes of the channel pairs whose sink was Fz first remained still and then declined at the point when the normalized RT was approximately 4 with the increased normalized RT. Furthermore, when we observed the frontal- and motor-related channel pairs, such as Fz-to-C3, Cz-to-Fz, C3-to-Fz, and C4-to-Fz, the connectivity magnitudes dropped sharply and reached the bottom at a normalized RT of 4. Compared to the similar declining trend in the connectivity magnitude in the normal and reduced states, the one in the high-risk state reached the bottom earlier than both of them. The inverted U-shape and inverted U-shaped shift were observed in both the reduced and normal states; however, we only observed similar patterns at channel pairs with Oz as their sink.

Overall, we found that the normalized reaction times in which the connectivity magnitude reached the lowest point gradually progressively moved from the high-risk state, the reduced state to the normal state in these channel pairs, such as Fz-to-C4, Cz-to-C4 and Oz-related pairs. Consider Cz-to-Oz, for example. The connectivity magnitude reached its lowest point when the reaction time was 6 in the normal state. The connectivity magnitude reached its lowest point when the reaction time was 5 in the reduced state. The connectivity magnitude reached its lowest point when the reaction time was 4 in the high-risk state.

C. Comparison of EEG Connectivity Changes Between Any Two Levels of Daily Fatigue

The comparisons of the connectivity magnitudes among the channel pairs among the three states (the high-risk, reduced, and normal state, respectively) are displayed in Figs. 4 and 6 (vertical axis, TE values between all channel pairs; horizontal axis, sorted normalized RTs), where causality is from row to column (Color: red, high-risk state; green, reduced state; and blue, normal state). All measures were smoothed using a window smoothing method (window size: 1 unit of RT; step size: 0.1 unit of RT). A Wilcoxon signed-rank test was used to test the pairwise comparisons between the TE values of each two states. We used the false discovery rate (FDR) to obtain the FDR-adjusted p-values. The black star '$*$' under each channel pair represents that the FDR-adjusted p-value was less than 0.05. The region of normalized reaction time where the black star ($*$) appeared represented that a significant difference between the TE values of the two states had been found. Fig. 4 compares the connectivity magnitudes in the high-risk and the reduced states. In addition to significant differences among Oz-related channel pairs, there were significant differences among Fz-related channel pairs. Furthermore, significant differences were found among motor-related channel pairs, such as C3-to-C4, and C4-to-Cz. It is clear from above that the short normalized reaction time was responsible for most of the significant differences between high-risk and reduced TE values.

Fig. 5 compares the connectivity magnitudes in the reduced and the normal states. Compared with the former results of the comparison between the high-risk state and the reduced state, significant differences were hardly found among the Oz-related channel pairs. Nevertheless, there were significant differences among the Fz-related pairs. The number of significant differences was less than that of the previous results among the motor-related pairs. In addition, most of the differences were found at the short normalized reaction time.

Fig. 6 compares the connectivity magnitudes in the high-risk and the normal state. There were significant differences among the pairs of Oz-related channels as well as between the pairs of FZ-related channels and motor-related channel pairs. Most of the differences were found at the short normalized reaction time. It was interesting to note that the results of the comparison between the normal and high-risk states were similar to the results of the comparison between the reduced and high-risk states.

In this study, we present the comparison of TE values between any two levels of daily fatigue. Integrating the results above can be concluded: First, the significant differences were found at the short normalized reaction time. Second, the connectivity changes in the high-risk state were clearly different from the changes in the reduced and normal states.

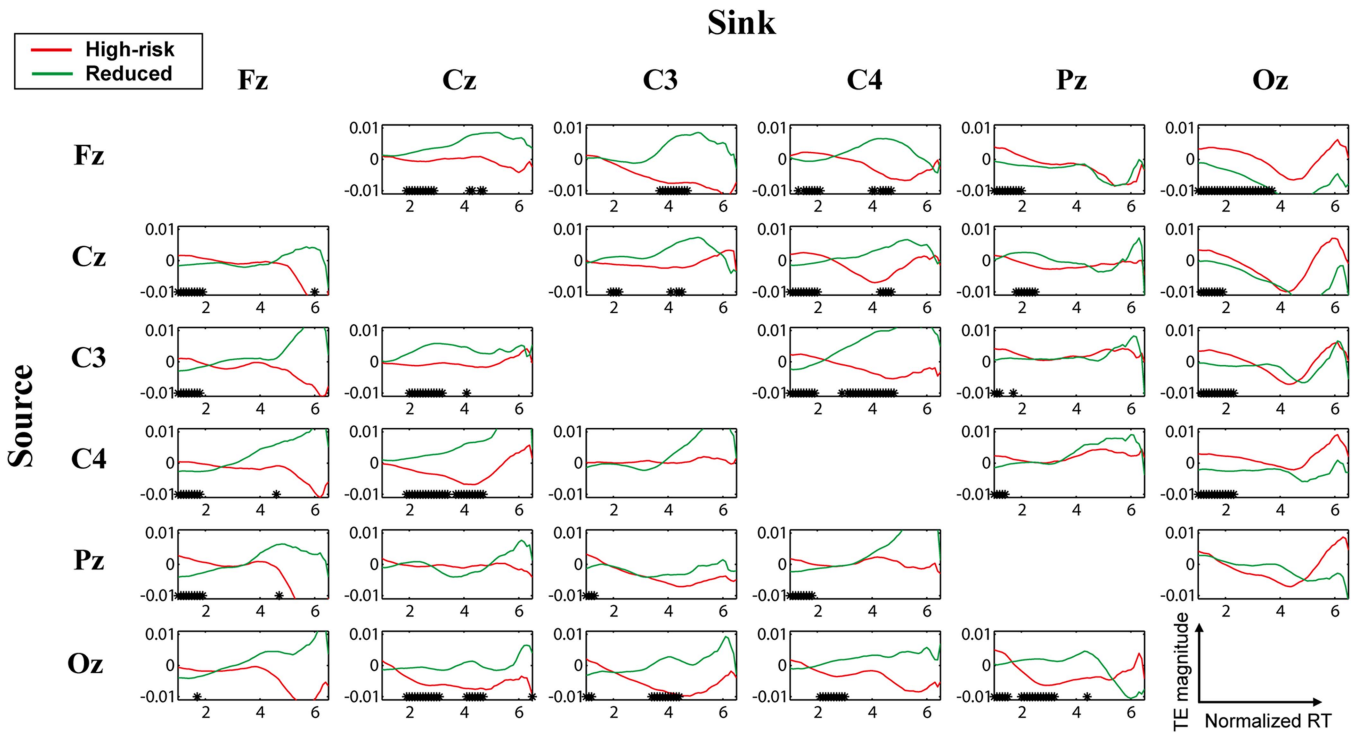

Fig. 4. Comparison of the connectivity magnitudes between the pairs of EEG channels (Fz, Cz, C3, C4, Pz, and Oz) in the high-risk and the reduced states. The red and green curves are high-risk and reduced groups. ∗FDR-adjusted p-value <0.05.

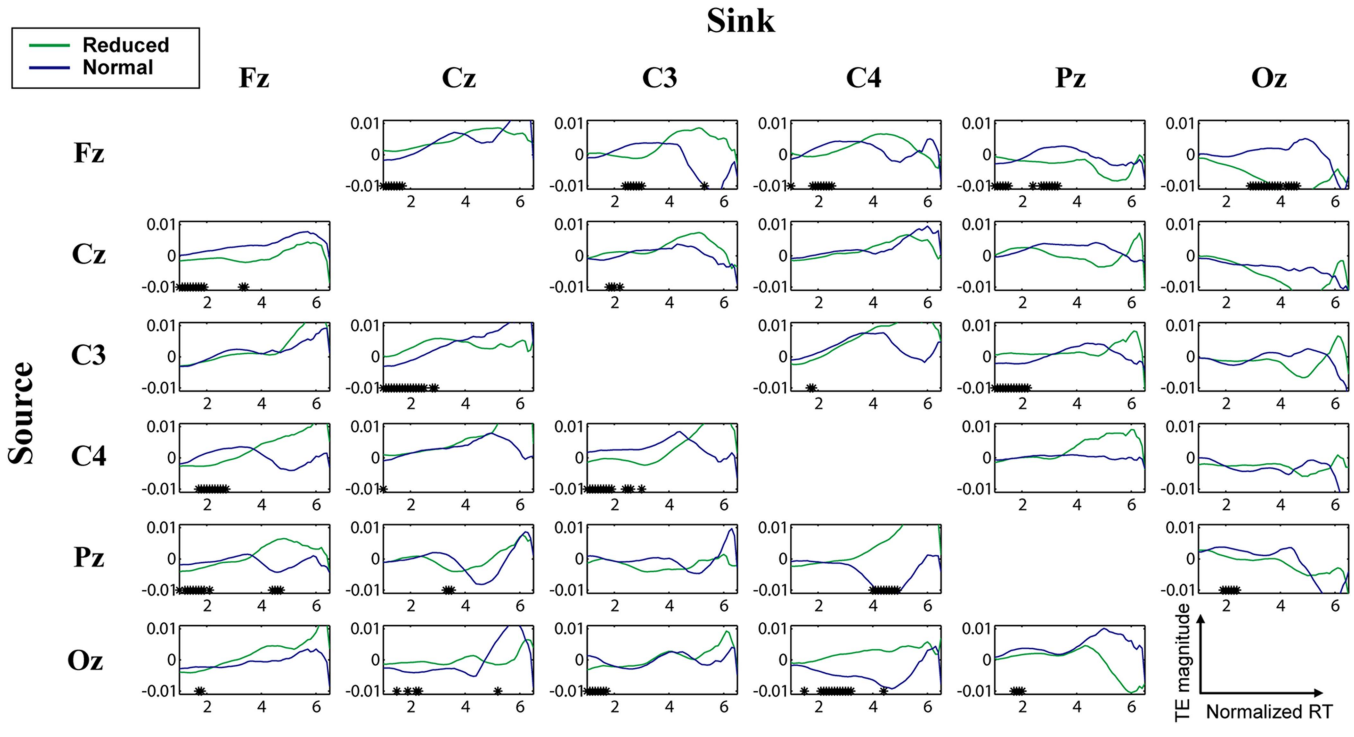

Fig. 5. Comparison of the connectivity magnitudes between the pairs of EEG channels (Fz, Cz, C3, C4, Pz, and Oz) in the reduced and the normal states. The green and blue curves are reduced and normal groups. ∗FDR-adjusted p-value <0.05.

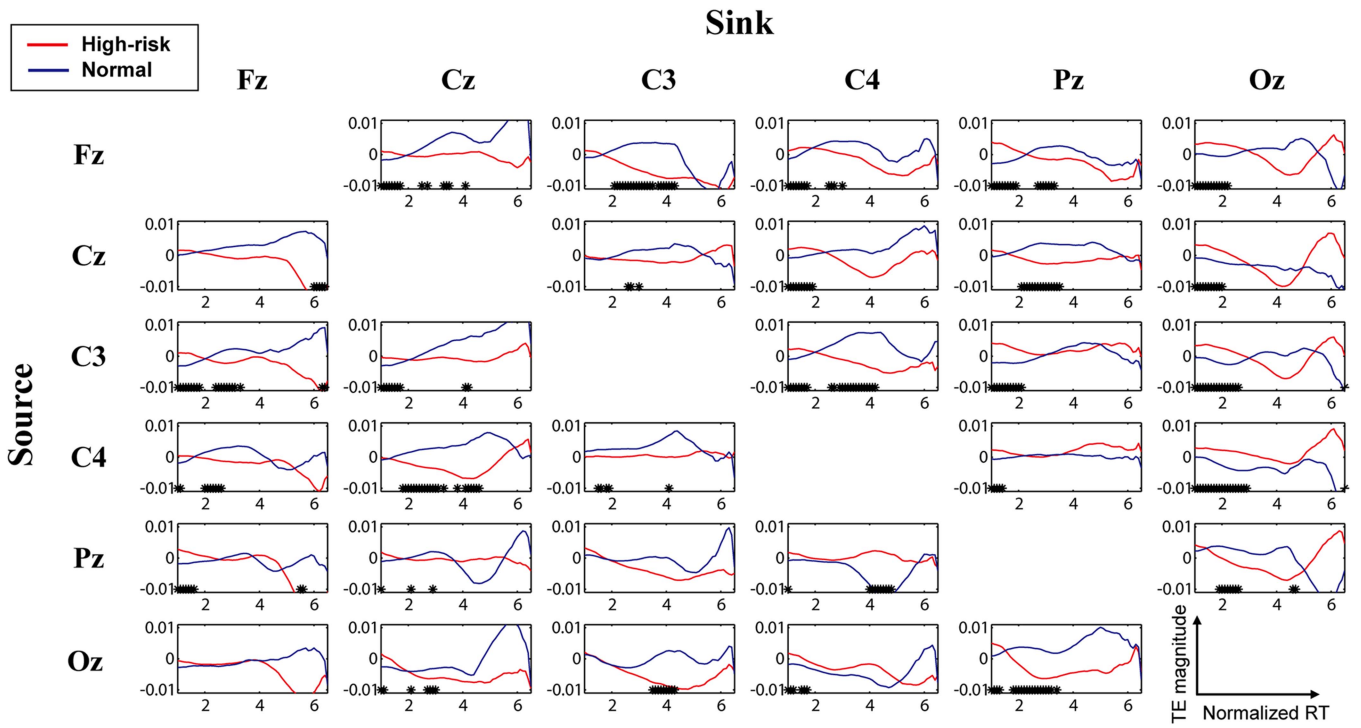

Fig. 6. Comparison of the connectivity magnitudes between the pairs of EEG channels (Fz, Cz, C3, C4, Pz, and Oz) in the high-risk and the normal state. The red and blue curves are high-risk and normal groups. ∗FDR-adjusted p-value <0.05.

The high-risk state and the normal state were the two extreme states among the levels of daily fatigue. Therefore, it would be vital and meaningful to inspect the difference between the connectivity magnitudes of the high-risk state and of the normal state in detail. Fig. 6 depicts the comparison of the connectivity changes between the high-risk state and the normal state. The black star '∗' under each cell represents that there was significant difference between the TE values of the two states at the particular normalized RT. The greater the number of black stars '∗' that appeared at the region of the RT, the greater the difference found in the TE values between the two states. We chose the region from normalized RT =1.5 to normalized RT ratio=3, which was the region that had the most black stars (∗) located in. In previous studies, the so-called fight fatigue phenomenon of subjects would occur at the interval of the normalized RT. The performance of subjects was suboptimal in this region of the normalized RT. The states of subjects were stationary at the region of the normalized RT. It was quite appropriate for us to use the region of the normalized RT to inspect the differences in the TE values between two states. The mean of the TE values in the region was calculated. Then, we subtracted the mean TE value of the high-risk state from the mean TE value of the normal state as the TE difference. This measure represented the strength of the link among any two chosen channel between the two states. Based on the calculation above, the difference in the TE values between the high-risk state and the normal state is shown in Fig. 7. We defined the difference magnitude by the normalization technique and the formula as follow:

$$\text{Magnitude ratio}: \frac{|\text{High-risk} - \text{Normal}|}{\min\left(|\text{High-risk} - \text{Normal}|\right)} \quad (5)$$

where "High-risk" represents the mean of the TE values in the high-risk state from RT=1.5 to RT=3, and "Normal" represents the mean of TE values in the normal state from RT=1.5 to RT=3. The red arrow indicates that the TE values in the high-risk state were higher than those in the normal state. This represented that the magnitude of the link between two chosen channels increased from the normal state to the high-risk state; the blue arrow meant that the TE value at the high-risk state was lower than the one at the normal state. It represented that the magnitude of link between two chosen channels decreased from the normal state to the high-risk state.

In the frontal region, most of the links were blue, which indicates that information flow decreased from the normal state to the high-risk state among channel pairs in the frontal region. On the other hand, in the occipital region, most of the links were red, indicating that the information flow increased among channel pairs from the normal state to the high-risk state.

IV. Discussion

A. Effect of Fatigue on TE Fluctuations During Driving

The results showed that the EEG connectivity fluctuated within a single level of daily fatigue. There was an inverted-U shaped change in the TE at several channel pairs. From great driving performance to poor driving performance, the subjects would feel tired gradually and suffered from declining alertness. However, they were asked to react to the deviation in the lane-keeping task as quickly as possible. Therefore, much more strength and effort were required for the participants to engage in the task. This resulted in the occurrence of an inverted-U shaped change in the TE. In the previous studies, there were

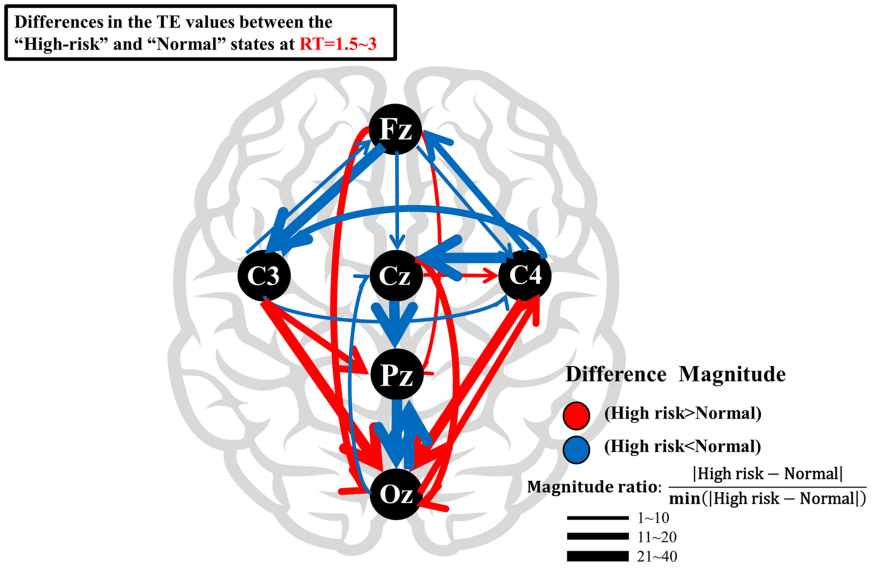

Fig. 7. Differences between the TE values of the high-risk state and the normal state. The red solid arrows indicate that the TE values of the high-risk state were higher than those of the normal states. The blue solid arrows indicate that the TE values of the normal state were higher than those of the high-risk state. The thickness of each arrow is divided into three levels to represent the three different magnitude levels (1–10, 11–20, and 21–40).

similar changes that occurred in the brain under sleep deprivation [25], [43]. Additional compensatory resources were needed to implement cognitive tasks or maintain the task performance via the enhancement of couplings [43], [44], [45], [46], [47], [48].

As driving performance was poor, subjects who reacted slowly to the environmental stimulus were possibly prone to be drowsy. The declining tendency of the connectivity magnitude that was observed at many channel pairs under each level of daily fatigue may be associated with the fading of consciousness [27], [49]. A cortical gate is created through the reductions in cortico-cortical connectivity, and it may disconnect the brain from the external environment and, thus, block sensory inputs [27], [50].

According to the results mentioned above, we found an inverted-U shaped change in the TE in the normal and reduced states. There were descending trends of the connectivity magnitudes in the normal, reduced and the high-risk states. In addition, we observed an inverted-U shaped shift in the change in the TE in the normal and reduced states. And there were different descending trends across the different levels of daily fatigue. Therefore, it was suggested that the result was different from those of the past studies [27].

Previous research [27], which was related to the brain dynamics during a driving task, also presented the relationship between connectivity and reaction time. The previous research did not separate the EEG data based on the current daily fatigue level of each subject as they conducted the task. The results indicated that inverted-U shaped changes in the TE values were observed in Fz-, Cz-, C3-, C4- and Pz-associated connectivity. In our study, we observed an inverted-U shaped change only in the normal and reduced states. In addition, an inverted-U shaped shift, a variant of the classical inverted U-shape, was observed at the Oz- associated channel pairs in the normal state and at the motor-related region in the reduced state. This type of inverted U-shape was different from the one that was presented in the previous research, and it was found only in this study. Additionally, subjects in high-risk states might feel tired and lose consciousness during driving tasks. Therefore, the descending shape of connectivity dominated most of the channel pairs, and there were no inverted-U shaped changes in the high-risk state. Our result not only aligned with those of the previous study but also presented a more significant number of different styles of connectivity fluctuations across the distinct groups. This finding suggested that different levels of daily fatigue actually affect the relationship between brain connectivity and behavior during drowsy driving.

Apart from this, previous research [27] showed a monotonic descending trend in the connectivity of the occipital area, especially in Pz-to-Oz, and Oz-to-Pz. In our study, we discovered different kinds of descending shapes of the connectivity magnitudes across the three distinct groups at the Fz-to-C4, Cz-to-C4 and Oz-related pairs. From the normal state, the reduced state to the high-risk state, the connectivity magnitude reached the bottom progressively earlier at these particular pairs. When the subjects were transitioning from a low-fatigue level to a high-fatigue level, they enter into a drowsy state wherein they were prone to feeling tired and making mistakes. Moreover, we found from the video that the high-risk group fell asleep during the driving task. As mentioned above, the descending tendency of the connectivity magnitude may be associated with the fading of consciousness [27], [49] and with the reductions in the cortico-cortical connectivity. Consequently, this gave rise to the finding that the drowsier the subjects were, the earlier the connectivity magnitude reached the bottom. In our study, we divided all the EEG data into three groups based on the different levels of daily fatigue, and we observed the fluctuations in the

connectivity changes. Hence, in contrast to the past research, we discovered some differences, such as the distinct types of descending trends among the groups, that certainly represented that different fatigue conditions change the subjects' brain-behavior relationships during driving.

B. Effect of Fatigue on TE Difference Between the High-Risk State and the Normal State

According to the results mentioned above, we found that the high-risk state and the normal state were the two extreme states among the different levels of daily fatigue. Therefore, we then observed the effect of fatigue on the differences in the TE values between two of the groups. We chose the region from RT=1.5 to RT=3 in every channel pair and subtracted the mean TE value of the high-risk state from the mean TE value of the normal state as the TE difference. Using the calculation above, we depicted the information link between any two channel pairs between these two states.

In Fig 7, we observed the amount and direction of the information flow among the different brain regions. The result revealed that the connectivity magnitude decreased in the frontal area from the normal state to the high-risk state. There were several studies could be found that had presented similar results after sleep deprivation. Previous research [51] stated the sleep deprivation led to a loss of connectivity in the frontal brain region. Additionally, a study [52] of investigating the effects of total sleep deprivation and recovery sleep in normal subjects discovered that sleep deprivation led to a relative decrease in the glucose metabolism of the frontal cortex. In this study, the high-risk group contained the subjects were at the high-fatigue level. We suspected that the subjects felt extremely tired and got into the high-fatigue level after the sleep deprivation. Hence, our results were similar to those of the existing studies.

As a result, from the normal state to the high-risk state, the occipital region was associated with a greater magnitude of connectivity. To maintain performance, subjects in the high-risk state must pay more attention to the driving task than subjects in the normal state. An increase in coherence magnitude in the parietal and occipital cortex is associated with sustained visual attention, as found in previous research [53]. Moreover, one of the studies [52] mentioned above suggested that sleep deprivation leads to a relative decrease in glucose metabolism in the frontal cortex but an increase in occipital activity. Compared with our findings, these studies showed similar results.

V. Conclusion

For this study, bio-data for each participant and effectiveness scores were recorded using the ReadiBand, a wrist-worn actigraphy device. As a result of the effectiveness score, the EEG data was divided into three levels of daily fatigue based on the subject's performance in lane-keeping tasks. Each subject was divided into three groups based on their levels of daily fatigue: the high-risk, reduced, and normal groups. Each subject's effective connectivity was determined by calculating the transfer entropy of the EEG data. Moreover, we observed brain connectivity fluctuations in all groups to determine whether acute fatigue, the progression from alert to drowsy, affected brain connectivity-behavior relationships.

As a result of the observations of brain connectivity fluctuations among the three groups, the results indicate that normal states and reduced states experienced changes in connectivity of some pairs of EEG channels in an inverted-U shape. In the high-risk state, however, no such findings were found. Additionally, we found different types of descending shapes in connectivity magnitudes among the three distinct groups. From the normal state, the reduced state to the high-risk state, the magnitude of connectivity reached the bottom progressively earlier at some particular pairs.

Moreover, we observed a difference in connectivity between normal and high-risk states after examining the RT-sorted connectivity changes. From the normal to the high-risk state, connectivity magnitude decreased in the frontal region. In addition, we found that connectivity magnitude increased in the occipital region from the normal to the high-risk state. In addition, the strength of the connectivity between the frontal and occipital cortical regions increased. In summary, this study revealed the variations in the magnitude of connectivity between the pairs of different brain regions among different levels of daily fatigue during drowsy driving.

Authors' Contributions

Chin-Teng Lin conceptualized and designed the study, performed data analysis, conducted critical revisions of the manuscript for important intellectual content, and approved the work. Kuan-Chih Huang designed the study, conducted experiment design, data collection, data analysis, statistical analysis, and contributed to the drafting and critical revision of the manuscript. Chun-Ying Tseng contributed to data analysis, statistical analysis, and manuscript drafting.

Conflict of Interest

The authors declare no conflict of interest.

References

[1] J. D. Lee, "Fifty years of driving safety research," *Hum. Factors*, vol. 50, no. 3, pp. 521–528, Jun. 2008.
[2] T. Taniguchi and A. Takaoka, "A weak signal for strong responses: Interferon-alpha/beta revisited," *Nature Rev. Mol. Cell Biol.*, vol. 2, no. 5, pp. 378–386, May 2001.
[3] A. Campagne, T. Pebayle, and A. Muzet, "Correlation between driving errors and vigilance level: Influence of the driver's age," *Physiol. Behav.*, vol. 80, no. 4, pp. 515–524, Jan. 2004.
[4] R.-S. Huang, T.-P. Jung, A. Delorme, and S. Makeig, "Tonic and phasic electroencephalographic dynamics during continuous compensatory tracking," *Neuroimage*, vol. 39, no. 4, pp. 1896–1909, 2008.
[5] R.-S. Huang, T.-P. Jung, and S. Makeig, "Tonic changes in EEG power spectra during simulated driving," in *Proc. Int. Conf. Found. Augmented Cogn.*, 2009, pp. 394–403.
[6] C. T. Lin et al., "Tonic and phasic EEG and behavioral changes induced by arousing feedback," *Neuroimage*, vol. 52, no. 2, pp. 633–642, Aug. 2010.
[7] C.-T. Lin, K.-C. Huang, C.-H. Chuang, L.-W. Ko, and T.-P. Jung, "Can arousing feedback rectify lapses in driving? Prediction from EEG power spectra," *J. Neural Eng.*, vol. 10, no. 5, 2013, Art. no. 056024.
[8] K. C. Huang et al., "An EEG-based fatigue detection and mitigation system," *Int. J. Neural Syst.*, vol. 26, no. 4, Jun. 2016, Art. no. 1650018.

[9] K. C. Huang, C. H. Chuang, Y. K. Wang, C. Y. Hsieh, J. T. King, and C. T. Lin, "The effects of different fatigue levels on brain-behavior relationships in driving," *Brain Behav.*, vol. 9, no. 12, Dec. 2019, Art. no. e01379.

[10] K. J. Friston, "Functional and effective connectivity in neuroimaging: A synthesis," *Hum. Brain Mapping*, vol. 2, no. 1/2, pp. 56–78, 1994.

[11] W. C. Liu, J. F. Flax, K. G. Guise, V. Sukul, and A. A. Benasich, "Functional connectivity of the sensorimotor area in naturally sleeping infants," *Brain Res.*, vol. 1223, pp. 42–49, Aug. 2008.

[12] R. Vicente, M. Wibral, M. Lindner, and G. Pipa, "Transfer entropy-a model-free measure of effective connectivity for the neurosciences," *J. Comput. Neurosci.*, vol. 30, no. 1, pp. 45–67, Feb. 2011.

[13] C. J. Werner et al., "Altered motor network activation and functional connectivity in adult Tourette's syndrome," *Hum. Brain Mapping*, vol. 32, no. 11, pp. 2014–2026, Nov. 2011.

[14] H. Wang et al., "Dynamic reorganization of functional connectivity unmasks fatigue related performance declines in simulated driving," *IEEE Trans. Neural Syst. Rehabil. Eng.*, vol. 28, no. 8, pp. 1790–1799, Aug. 2020.

[15] C. Chen, Z. Ji, Y. Sun, A. Bezerianos, N. Thakor, and H. Wang, "Self-attentive channel-connectivity capsule network for EEG-based driving fatigue detection," *IEEE Trans. Neural Syst. Rehabil. Eng.*, vol. 31, pp. 3152–3162, 2023.

[16] H. Wang, L. Xu, A. Bezerianos, C. Chen, and Z. Zhang, "Linking attention-based multiscale CNN with dynamical GCN for driving fatigue detection," *IEEE Trans. Instrum. Meas.*, vol. 70, 2021, Art. no. 2504811.

[17] A. Korzeniewska, M. Manczak, M. Kaminski, K. J. Blinowska, and S. Kasicki, "Determination of information flow direction among brain structures by a modified directed transfer function (dDTF) method," *J. Neurosci. Methods*, vol. 125, no. 1/2, pp. 195–207, May 2003.

[18] K. J. Blinowska, R. Kus, and M. Kaminski, "Granger causality and information flow in multivariate processes," *Phys. Rev. E*, vol. 70, no. 5, Nov. 2004, Art. no. 050902.

[19] L. Astolfi et al., "Comparison of different cortical connectivity estimators for high-resolution EEG recordings," *Hum. Brain Mapping*, vol. 28, no. 2, pp. 143–157, Feb. 2007.

[20] J. Cao et al., "Brain functional and effective connectivity based on electroencephalography recordings: A review," *Hum. Brain Mapping*, vol. 43, no. 2, pp. 860–879, 2022.

[21] C. W. J. Granger, "Investigating causal relations by econometric models and cross-spectral methods," *Econometrica*, vol. 37, no. 3, pp. 424–438, 1969.

[22] G. N. Dimitrakopoulos et al., "Functional connectivity analysis of mental fatigue reveals different network topological alterations between driving and vigilance tasks," *IEEE Trans. Neural Syst. Rehabil. Eng.*, vol. 26, no. 4, pp. 740–749, Apr. 2018.

[23] F. Wang, S. Wu, J. Ping, Z. Xu, and H. Chu, "EEG driving fatigue detection with PDC-based brain functional network," *IEEE Sensors J.*, vol. 21, no. 9, pp. 10811–10823, May 2021.

[24] O. Friman, J. Cedefamn, P. Lundberg, H. Borga, and H. Knutsson, "Detection of neural activity in functional MRI using canonical correlation analysis," *Magn. Reson. Med.*, vol. 45, no. 2, pp. 323–330, Feb. 2001.

[25] P. von Bunau, F. C. Meinecke, F. C. Kiraly, and K. R. Muller, "Finding stationary subspaces in multivariate time series," *Phys. Rev. Lett.*, vol. 103, no. 21, Nov. 2009, Art. no. 214101.

[26] T. Schreiber, "Measuring information transfer," *Phys. Rev. Lett.*, vol. 85, no. 2, pp. 461–464, Jul. 2000.

[27] C. S. Huang, N. R. Pal, C. H. Chuang, and C. T. Lin, "Identifying changes in EEG information transfer during drowsy driving by transfer entropy," *Front. Hum. Neurosci.*, vol. 9, Oct. 2015, Art. no. 570.

[28] T.-P. Jung, S. Makeig, M. J. McKeown, A. J. Bell, T.-W. Lee, and T. J. Sejnowski, "Imaging brain dynamics using independent component analysis," *Proc. IEEE*, vol. 89, no. 7, pp. 1107–1122, Jul. 2001.

[29] S. Olbrich et al., "EEG-vigilance and BOLD effect during simultaneous EEG/fMRI measurement," *Neuroimage*, vol. 45, no. 2, pp. 319–332, Apr. 2009.

[30] S. W. Chuang, L. W. Ko, Y. P. Lin, R. S. Huang, T. P. Jung, and C. T. Lin, "Co-modulatory spectral changes in independent brain processes are correlated with task performance," *Neuroimage*, vol. 62, no. 3, pp. 1469–1477, Sep. 2012.

[31] P. G. Samann et al., "Increased sleep pressure reduces resting state functional connectivity," *Magn. Reson. Mater. Phys. Biol. Med.*, vol. 23, no. 5/6, pp. 375–389, Dec. 2010.

[32] J. A. De Havas, S. Parimal, C. S. Soon, and M. W. L. Chee, "Sleep deprivation reduces default mode network connectivity and anti-correlation during rest and task performance," *Neuroimage*, vol. 59, no. 2, pp. 1745–1751, Jan. 2012.

[33] B. T. T. Yeo, J. Tandi, and M. W. L. Chee, "Functional connectivity during rested wakefulness predicts vulnerability to sleep deprivation," *Neuroimage*, vol. 111, pp. 147–158, May 2015.

[34] T. Åkerstedt and M. Gillberg, "Subjective and objective sleepiness in the active individual," *Int. J. Neurosci.*, vol. 52, no. 1/2, pp. 29–37, 1990.

[35] G. Kecklund and T. Åkerstedt, "Sleepiness in long distance truck driving: An ambulatory EEG study of night driving," *Ergonomics*, vol. 36, no. 9, pp. 1007–1017, 1993.

[36] K. A. Lee, G. Hicks, and G. Nino-Murcia, "Validity and reliability of a scale to assess fatigue," *Psychiatry Res.*, vol. 36, no. 3, pp. 291–298, 1991.

[37] S. R. Hursh et al., "Fatigue models for applied research in warfighting," *Aviation Space Environ. Med.*, vol. 75, no. 3, pp. A44–A53, Mar. 2004.

[38] A. Kraskov, H. Stogbauer, and P. Grassberger, "Estimating mutual information," *Phys. Rev. E*, vol. 69, no. 6, Jun. 2004, Art. no. 066138.

[39] K. Hlavackova-Schindler, M. Palus, M. Vejmelka, and J. Bhattacharya, "Causality detection based on information-theoretic approaches in time series analysis," *Phys. Rep.-Rev. Sect. Phys. Lett.*, vol. 441, no. 1, pp. 1–46, Mar. 2007.

[40] M. Lindner, R. Vicente, V. Priesemann, and M. Wibral, "TRENTOOL: A Matlab open source toolbox to analyse information flow in time series data with transfer entropy," *BMC Neurosci.*, vol. 12, pp. 1–22, Nov. 2011.

[41] L. Y. Cao, "Practical method for determining the minimum embedding dimension of a scalar time series," *Physica D: Nonlinear Phenomena*, vol. 110, no. 1/2, pp. 43–50, Dec. 1997.

[42] M. Ragwitz and H. Kantz, "Markov models from data by simple nonlinear time series predictors in delay embedding spaces," *Phys. Rev. E*, vol. 65, no. 5, pp. 43–50, May 2002.

[43] W. Szelenberger, T. Piotrowski, and A. J. Dabrowska, "Increased prefrontal event-related current density after sleep deprivation," *Acta Neurobiologiae Experimentalis*, vol. 65, no. 1, pp. 19–28, 2005.

[44] C. M. Portas, G. Rees, A. M. Howseman, O. Josephs, R. Turner, and C. D. Frith, "A specific role for the thalamus in mediating the interaction of attention and arousal in humans," *J. Neurosci.*, vol. 18, no. 21, pp. 8979–8989, Nov. 1998.

[45] S. P. A. Drummond, G. G. Brown, J. C. Gillin, J. L. Stricker, E. C. Wong, and R. B. Buxton, "Altered brain response to verbal learning following sleep deprivation," *Nature*, vol. 403, no. 6770, pp. 655–657, Feb. 2000.

[46] S. P. A. Drummond and G. G. Brown, "The effects of total sleep deprivation on cerebral responses to cognitive performance," *Neuropsychopharmacology*, vol. 25, pp. S68–S73, Nov. 2001.

[47] S. P. A. Drummond, J. C. Gillin, and G. G. Brown, "Increased cerebral response during a divided attention task following sleep deprivation," *J. Sleep Res.*, vol. 10, no. 2, pp. 85–92, Jun. 2001.

[48] S. P. A. Drummond, G. G. Brown, J. S. Salamat, and J. C. Gillin, "Increasing task difficulty facilitates the cerebral compensatory response to total sleep deprivation," *Sleep*, vol. 27, no. 3, pp. 445–451, May 2004.

[49] M. Massimini, F. Ferrarelli, R. Huber, S. K. Esser, H. Singh, and G. Tononi, "Breakdown of cortical effective connectivity during sleep," *Science*, vol. 309, no. 5744, pp. 2228–2232, Sep. 2005.

[50] S. K. Esser, S. Hill, and G. Tononi, "Breakdown of effective connectivity during slow wave sleep: Investigating the mechanism underlying a cortical gate using large-scale modeling," *J. Neurophysiol.*, vol. 102, no. 4, pp. 2096–2111, Oct. 2009.

[51] I. M. Verweij, N. Romeijn, D. J. A. Smit, G. Piantoni, E. J. W. Van Someren, and Y. D. van der Werf, "Sleep deprivation leads to a loss of functional connectivity in frontal brain regions," *BMC Neurosci.*, vol. 15, pp. 1–10, Jul. 2014.

[52] J. C. Wu et al., "Frontal lobe metabolic decreases with sleep deprivation not totally reversed by recovery sleep," *Neuropsychopharmacology*, vol. 31, 2006, Art. no. 2783.

[53] T. Z. Lauritzen, M. D'Esposito, D. J. Heeger, and M. A. Silver, "Top-down flow of visual spatial attention signals from parietal to occipital cortex," *J. Vis.*, vol. 9, no. 13, p. 18, 2009.